(for Handbook on Electron Transfer in Chemistry)

REFLECTIONS ON THE TWO-STATE ELECTRON TRANSFER MODEL

BRUCE S. BRUNSCHWIG AND NORMAN SUTIN

Chemistry Department, Brookhaven National Laboratory, Upton, New York 11973-5000

CONTENTS

I. INTRODUCTION

There is general agreement that the two most important factors determining electron transfer rates in solution are the degree of electronic interaction between the donor and acceptor sites, and the changes in the nuclear configurations of the donor, acceptor, and surrounding medium that occur upon the gain or loss of an electron [1-5]. The electronic interaction of the sites will be very weak, and the electron transfer slow, when the sites are far apart or their interaction is symmetry or spin forbidden. Since electron motion is much faster than nuclear motion, energy conservation requires that, prior to the actual electron transfer, the nuclear configurations of the reactants and the surrounding medium adjust from their equilibrium values to a configuration (generally) intermediate between that of the reactants and products. In the case of electron transfer between two metal complexes in a polar solvent, the nuclear configuration changes involve adjustments in the metal-ligand and intraligand bond lengths and angles, and changes in the orientations of the surrounding solvent molecules. In common with ordinary chemical reactions, an electron transfer reaction can then be described in terms of the motion of the system on an energy surface from the reactant equilibrium configuration (initial state) to the product equilibrium configuration (final state) via the activated complex (transition state) configuration.

This chapter will focus on the predictions of the traditional two-state electron transfer model. Only the ground and lowest excited state of the system are considered and contributions from higher electronic states are ignored. Thermal and optical electron transfers in both weakly and strongly interacting systems are discussed. The treatment is not intended to be exhaustive but instead will focus on certain features of the model that may be less familiar but which nevertheless have important implications.

II. ZERO-ORDER ENERGY SURFACES

Provided a hypothetical change in the charge on the reactants produces a proportional change in the dielectric polarization of the surrounding medium, the distortions of the reactants and products from their equilibrium configurations can be described in terms of diplacements on harmonic free-energy curves with identical force constants [1-5]. This is illustrated in Figures 1 and 2 where the free energy of the close-contact reactants plus surrounding medium (Curve G_a) and the free energy of the close-contact products plus surrounding medium (Curve G_b) are plotted vs. the reaction coordinate for a self-exchange reaction. The free-energy curves depict the zero-order or diabatic states of the system. Figure 1 shows the diabatic free-energy curves for a self-exchange reaction (Eq. (2.1a), $\Delta G^o = 0$) and Figure 2 the curves for an electron transfer reaction accompanied by a net chemical change (Eq. (2.1b), $\Delta G^o < 0$ for an exergonic reaction).

$$Fe(H_2O)_6^{2+} + Fe(H_2O)_6^{3+} = Fe(H_2O)_6^{3+} + Fe(H_2O)_6^{2+} \quad (2.1a)$$

$$Fe(H_2O)_6^{2+} + Ru(bpy)_3^{3+} = Fe(H_2O)_6^{3+} + Ru(bpy)_3^{2+} \quad (2.1b)$$

The curves have identical force constants f and their minima are separated by a_o. The vertical difference between the free energies of the reactants and products of a self-exchange reaction at the reactants' (or products') minimum (equilibrium configuration) is the reorganization parameter $\lambda = fa_o^2/2$. Denoting the displacement along the reaction coordinate by x, a dimensionless reaction coordinate X may be defined as x/a_o: X varies from 0 to 1 as the reaction proceeds and, with X as the coordinate, the force constants of the parabolas are equal to 2λ.

$$G_a = \frac{f}{2}x^2 = \lambda X^2 \quad (2.2a)$$

$$G_b = \frac{f}{2}(x - a_o)^2 + \Delta G^o = \lambda(X-1)^2 + \Delta G^o \quad (2.2b)$$

The sum and difference of the zero-order free energies are given by

$$(G_b + G_a) = 2\lambda(X - 1/2)^2 + 1/2 + \Delta G^o \quad (2.3a)$$

$$(G_b - G_a) = \lambda(1 - 2X) + \Delta G^o \quad (2.3b)$$

and the free-energy curves defined by these equations are included in Figures 1 and 2. The sum of the free energies of the reactants and products is a parabola[6] with force constant 4λ centered at $X = 1/2$ with its minimum vertically displaced relative to the reactant minimum by $\lambda/2 + \Delta G^o$. Similarly, the dependence of the average diabatic energy $(G_b + G_a)/2$ on X also is harmonic but with force constant 2λ, identical to that of the separated reactants and product curves. The parabola defined by the average energies *is still centered at $X = 1/2$* but with its minimum vertically displaced relative to the reactant minimum by $\lambda/4 + \Delta G^o/2$. Since the difference between the diabatic free-energies of the reactants and products $(G_b - G_a)$ is linearly related to X, this difference affords a measure of the progress of the reaction [7, 8] and, as a consequence, it provides an alternate definition of the reaction coordinate. For both self-exchange reactions and reactions accompanied by a net chemical change, the slope of $(G_b - G_a)$ vs. X is equal to -2λ.

The free energy of activation for the electron transfer is the difference between the free energies of the transition-state configuration and the equilibrium configuration of the reactants.

$$\Delta G^* = G_X^* - G_{a,eq} \quad (2.4)$$

The equilibrium configuration of the reactants in the zero-interaction limit is located at $X = 0$ with $G_{a,eq} = 0$. At the transition state, $G_a^* = G_b^*$ so that X^* and the free energy of activation in the zero-interaction limit are given by Eqs. (2.5a) and (2.5b), respectively.

$$X^* = \frac{1}{2}\left(1 + \frac{\Delta G^o}{\lambda}\right) \tag{2.5a}$$

$$\Delta G^* = \lambda (X^*)^2 = \frac{\lambda}{4}\left(1 + \frac{\Delta G^o}{\lambda}\right)^2 \tag{2.5b}$$

Evidently $\Delta G^* = \lambda/4$ for $\Delta G^o = 0$. Three free-energy regimes can be distinguished depending on the relative magnitudes of λ and ΔG^o. When $-\Delta G^o < \lambda$ the reaction is in the normal regime where ΔG^* decreases, and the rate constant increases, with increasing driving force. The reaction becomes barrierless ($\Delta G^* = 0$) when $-\Delta G^o = \lambda$ and ΔG^* is then insensitive to changes in ΔG^o. If the driving force is increased even further then $-\Delta G^o > \lambda$ and ΔG^* increases, and the rate constant decreases, with increasing driving force. This is the counter-intuitive inverted regime.

By using the Gibbs-Helmholtz equations, it follows from Eq. (2.5b) that the activation enthalpy and entropy are given by:

$$\Delta H^* = \frac{\Delta H_\lambda}{4}\left[1 - \left(\frac{\Delta G^0}{\lambda}\right)^2\right] + \frac{\Delta H^0}{2}\left(1 + \frac{\Delta G^0}{\lambda}\right) \tag{2.6a}$$

$$\Delta S^* = \frac{\Delta S_\lambda}{4}\left[1 - \left(\frac{\Delta G^0}{\lambda}\right)^2\right] + \frac{\Delta S^0}{2}\left(1 + \frac{\Delta G^0}{\lambda}\right) \tag{2.6b}$$

where $\Delta H_\lambda = \partial(\lambda/T)/\partial(1/T)$ and $\Delta S_\lambda = -\partial(\lambda)/\partial(T)$ [9]. Equation (2.5b) for the free energy of activation can be rewritten as

$$\Delta G^* = \frac{\lambda}{4}\left[1 - \left(\frac{\Delta G^0}{\lambda}\right)^2\right] + \frac{\Delta G^0}{2}\left(1 + \frac{\Delta G^0}{\lambda}\right) \tag{2.6c}$$

which is the same form as the activation enthalpy and entropy expressions.

The above equations give the activation parameters derived for the classical model. Departures are expected, and observed, for nonparabolic surfaces that are very weakly coupled and/or when the experimental activation parameters contain contributions from other sources [10].

III. SEMICLASSICAL TREATMENT

Electronic interaction of the reactants gives rise to the first-order energy surfaces shown as G_1 and G_2 in Figure 3. The splitting at the intersection of the zero-order energy surfaces in Figure 3 is equal to $2H_{ab}$, where H_{ab} is the electronic matrix element. We will treat H_{ab} as a positive quantity.

A. First-Order Energy Surfaces

If Ψ_a and Ψ_b denote the wave functions of the zero-order initial (reactant) and final (product) states, their interaction gives rise to two linear combinations, the first-order or adiabatic states

$$\Psi_1 = c_a\Psi_a + c_b\Psi_b \tag{2.6a}$$

$$\Psi_2 = c_a\Psi_b - c_b\Psi_a \tag{2.6b}$$

where Ψ_1 is the wave function for the lower (ground) and Ψ_2 is the wave function for the upper (excited) adiabatic state (energies G_1 and G_2, respectively) when the overlap integral S_{ab} is neglected (or is zero by construction [11]), and the mixing coefficients are normalized, i.e., $c_a^2 + c_b^2 = 1$. The energies of the adiabatic states are obtained by solving the two-state secular determinant

$$\begin{vmatrix} G_a - G & H_{ab} \\ H_{ab} & G_b - G \end{vmatrix} = 0 \tag{2.7}$$

where, as before, $G_a = H_{aa} = \langle\Psi_a|H|\Psi_a\rangle$ and $G_b = H_{bb} = \langle\Psi_b|H|\Psi_b\rangle$ are the energies of the diabatic states. H is the total Hamiltonian operator of the system including the interaction terms. The roots of the determinant are

$$G_1 = \frac{1}{2}\left\{\left(G_b + G_a\right) - \left[\left(G_b - G_a\right)^2 + 4H_{ab}^2\right]^{1/2}\right\} \tag{2.8a}$$

$$G_2 = \frac{1}{2}\left\{\left(G_b + G_a\right) + \left[\left(G_b - G_a\right)^2 + 4H_{ab}^2\right]^{1/2}\right\} \tag{2.8b}$$

The difference between the adiabatic energies is given by Eq. (2.9) while their sum is given by Eq. (2.10).

$$\left(G_2 - G_1\right) = \left[\left(G_b - G_a\right)^2 + 4H_{ab}^2\right]^{1/2} \tag{2.9a}$$

$$= \lambda\left[\left(1-2X+\frac{\Delta G^0}{\lambda}\right)^2+4\frac{H_{ab}^2}{\lambda^2}\right]^{1/2} \quad (2.9b)$$

$$\left(G_2+G_1\right)=\left(G_b+G_a\right) \quad (2.10a)$$

$$=\frac{\lambda}{2}\left[\left(2X-1\right)^2+1\right]+\Delta G^0 \quad (2.10b)$$

Evidently the average adiabatic energy $(G_2 + G_1)/2$, like the average diabatic energy, is described by a parabola with force constant 2λ centered at $X = 1/2$ with its minimum vertically displaced by $\lambda/4 + \Delta G^o/2$ relative to the diabatic minimum.

The product of the adiabatic energies is given by Eq. (2.11a), the product of the mixing coefficients is given by Eq. (2.11b), and $(1 - 2c_b^2)$ is given by Eq. (2.11c) [11].

$$G_1G_2 = G_aG_b - H_{ab}^2 \quad (2.11a)$$

$$c_ac_b = H_{ab}/(G_2 - G_1) \quad (2.11b)$$

$$\left(1-2c_b^2\right)=\left(\frac{G_b-G_a}{G_2-G_1}\right) \quad (2.11c)$$

The dependence of c_b^2 on the reaction coordinate is given by

$$c_b^2=\frac{1}{2}\left[1-\frac{(1-2X)}{\left\{\left[(1-2X)+\Delta G^0/\lambda\right]^2+4H_{ab}^2/\lambda^2\right\}^{1/2}}\right] \quad (2.12)$$

The squares of c_a and c_b are the fraction of the charge of the transferring electron that is on the donor and acceptor, respectively, at any given nuclear configuration. Thus c_b^2 also provides a measure of the progress of the electron transfer. *However, unlike X, which is a nuclear configuration coordinate, c_b^2 is an electronic configuration coordinate.* Figure 6 shows plots of c_b^2 vs X for various values of H_{ab}/λ. As is evident from Eq. (2.12) and Figure 6, the two coordinates are not linearly related except at very large H_{ab}. In the very weak interaction limit (diabatic curves, $H_{ab} = 0$) no electron density is transferred until $X = 0.5$ when the electron "suddenly" jumps from the donor to the acceptor. In this case c_b^2 is not a continuous function of X: instead $c_b^2 = 0$ for all $X < 1/2$ and $c_b^2 = 1$ for $X > 1/2$. As H_{ab} increases, charge density is transferred more gradually (with more delocalization present in the initial reactant configuration) and c_b^2 approaches linearity in X when $H_{ab} \geq \lambda$.

1. Symmetrical Systems

As shown in Figure 3, the splitting at the intersection of the diabatic energy curves lowers the barrier by H_{ab}. Further, as H_{ab} increases, the reactant and product minima of the adiabatic curves move closer together. The positions of the minima (reactant's and product's equilibrium configurations) are given by

$$X_{min,a} = \frac{1}{2}\left[1 - \left(1 - \frac{4H_{ab}^2}{\lambda^2}\right)^{1/2}\right] \tag{2.13a}$$

$$X_{min,b} = \frac{1}{2}\left[1 + \left(1 - \frac{4H_{ab}^2}{\lambda^2}\right)^{1/2}\right] \tag{2.13b}$$

and their energies are lowered by H_{ab}^2/λ relative to the diabatic minima [4]. In view of these changes the free energy of activation for a self-exchange reaction with appreciable coupling of the reactants is given by

$$\Delta G^* = \lambda/4 - H_{ab} + H_{ab}^2/\lambda \tag{2.14a}$$

$$= \frac{\lambda}{4}\left(1 - \frac{2H_{ab}}{\lambda}\right)^2 \tag{2.14b}$$

The second and third terms on the RHS of Eq. (2.14a) are due to the lowering of the barrier and the stabilization of the reactants, respectively [4].

Three classes of symmetrical systems may be distinquished depending on the magnitude of the electronic coupling of the donor and acceptor sites [12-14]. In Class I systems the coupling is very weak (Figure 1) and the properties of Class I systems are essentially those of the separate reactants (i.e., the adiabatic energy curves are very close to the diabatic curves). Activated electron transfer either does not occur at all or it occurs only very slowly (because of its high nonadiabaticity) with $\Delta G^* = \lambda/4$ and optical electron transfer can not occur Class II systems ($0 < H_{ab} < \lambda/2$, Figure 3) possess new optical and electronic properties in addition to those of the separate reactants. They remain valence trapped or charge localized: the electron transfers range from nonadiabatic ($H_{ab} < 10$ cm^{-1}) to strongly adiabatic ($H_{ab} > 200$ cm^{-1}) with ΔG^* given by Eq. (2.14). Equations (2.13) and (2.14) hold as long as the self-exchange reaction is described by a double well potential, i.e., as long as the system remains valence trapped. In Class

III systems the interaction of the donor and acceptor sites has become so large that two separate minima are no longer discernible and the lower energy surface features a single well at $X = 1/2$ (Figure 4). This is the delocalized case which occurs when $H_{ab} \geq \lambda/2$. The latter condition follows readily from the zero barrier limit ($\Delta G^* = 0$) of Eq. (2.14).

From Eq. (2.3b) the vertical difference between the *diabatic* energies at the equilibrium configuration (adiabatic minimum) of the reactants is given by

$$(G_b - G_a)_{eq} = \lambda(1 - 2X_{min}) \tag{2.15a}$$

$$= \lambda\left(1 - \frac{4H_{ab}^2}{\lambda^2}\right)^{1/2} \tag{2.15b}$$

It therefore follows from Eq. (2.9a) that the vertical difference between the adiabatic energies at the reactants' equilibrium configuration is given by

$$(G_2 - G_1)_{eq} = \lambda \tag{2.16}$$

This result is independent of H_{ab} for $H_{ab} \leq \lambda/2$. In other words, the vertical difference between the free energies of the reactants and products of a symmetrical reaction remains equal to λ at the equilibrium configuration of the reactants (or products) *regardless of the magnitude of the electronic coupling* as long as the system remains valence trapped [11]. Although the repulsion of the reactant and product curves increases with increasing H_{ab}, this is compensated for by the reactant and product minima moving closer together [15]. The net effect is that the adiabatic energy difference at X_{min} remains equal to λ.

It follows from Eqs. (2.11c) and (2.16) that, for $H_{ab} \leq \lambda/2$, $(c_b^2)_{eq}$ is given by

$$(c_b^2)_{eq} = \frac{1}{2}\left[1 - \left(1 - \frac{4H_{ab}^2}{\lambda^2}\right)^{1/2}\right] \tag{2.17}$$

Comparison with Eq. (2.13a) shows that, for a symmetrical system with $H_{ab} > 0$, $(c_b^2)_{eq} = X_{min,a}$. For $H_{ab}/\lambda = 0.3$ this corresponds to $X_{min,a} = 0.10$. Moreover, at the transition state for a symmetrical system $c_b^2 = X^* = 1/2$. The equilibrium and transition-state configurations are the only configurations at which X and c_b^2 for a symmetrical system are equal.

Values of $(G_2 - G_1)/\lambda$ calculated from Eq. (2.9b) are plotted vs X for various H_{ab}/λ values in Figure 5. The adiabatic energy difference flattens with increasing H_{ab} and becomes essentially independent of X when $H_{ab} \geq 2\lambda$. Under these conditions the system is deeply into the Class III

regime. Further, it is evident from Eq. (2.8) that, except for extreme values of X, the force constants of the vertically aligned *adiabatic* surfaces in very strongly coupled symmetrical systems ($H_{ab} \geq 2\lambda$) are equal to that of the original *diabatic* parabolas (cf discussion of Eq. (2.10)). Figure 6 shows that for typical symmetrical Class II systems most of the charge density is transferred between $X = 0.4$ - 0.6.

2. Unsymmetrical Systems

As in the case of symmetrical systems, the properties of an unsymmetrical Class I system are essentially those of the separate reactants. Although Class II systems are valence trapped, sufficiently endergonic reactions can exhibit a single minimum close to the noninteracting reactant minimum. This minimum shifts to $X^* = 0.5$ only when H_{ab} becomes very large. Provided that $H_{ab} < (\lambda + \Delta G^o)/2$ and $|\Delta G^o| < \lambda$, the positions of the reactant and product minima are given by Eqs. (2.18a) and (2.18b), while the location of the transition state is given by Eq. (2.18c).

$$X_{\text{min,a}} = \frac{H_{ab}^2/\lambda^2}{(1+\Delta G^o/\lambda)^2} \tag{2.18a}$$

$$X_{\text{min,b}} = 1 - \frac{H_{ab}^2/\lambda^2}{(1-\Delta G^o/\lambda)^2} \tag{2.18b}$$

$$X^* = \frac{\left(1+\Delta G^o/\lambda - 2H_{ab}/\lambda\right)}{2\left(1-2H_{ab}/\lambda\right)} \tag{2.18c}$$

The free energy of activation is given by

$$\Delta G^* = \frac{\lambda}{4} + \frac{\Delta G^o}{2} + \frac{(\Delta G^o)^2}{4(\lambda - 2H_{ab})} - H_{ab} + \frac{H_{ab}^{\ 2}}{(\lambda + \Delta G^o)} \tag{2.19}$$

In the above equations $-\Delta G^o$ is the driving force in the *noninteracting* ($H_{ab} = 0$) system [15].

B. Rate Constant Expressions

The first-order rate constant for intramolecular electron transfer or for electron transfer within the precursor complex formed from the reactants in a bimolecular reaction is given by

$$k_{el} = \kappa_{el} \nu_n \exp(-\Delta G^*/RT) \tag{3.1}$$

where κ_{el} is the electronic transmission coefficient, ν_n is the nuclear vibration frequency that takes the system through the intersection region and ΔG^* is the free energy of activation for the electron transfer [4].

The electronic transmission coefficient is the probability that electron transfer will occur once the system has reached the intersection region (transition state). Provided that the electronic interaction of the reactants is sufficiently strong $\kappa_{el} \approx 1$ and the electron transfer will occur with near unit probability in the intersection region: the electron transfer reaction is *adiabatic* with the system remaining on the lower energy surface on passing through the intersection region. Under these conditions k_{el} is given by

$$k_{el} = \nu_n \exp(-\Delta G^*/RT) \tag{3.2}$$

On the other hand, for a *nonadiabatic* reaction, $\kappa_{el} << 1$, $\kappa_{el}\nu_n = \nu_{el}$ and the rate constant is given by Eq. (3.3) where ν_{el} is the electron hopping frequency in the activated complex. The Landau-Zener treatment yields Eq. (3.4) for ν_{el} [16, 17].

$$k_{el} = \nu_{el} \exp(-\Delta G^*/RT) \tag{3.3}$$

$$\nu_{el} = \frac{2H_{ab}^2}{h}\left(\frac{\pi^3}{\lambda RT}\right)^{1/2} \tag{3.4}$$

In effect, the adiabatic and nonadiabatic limits of the transition state formalism correspond to $\nu_{el} >> \nu_n$ and $\nu_{el} << \nu_n$, respectively.

The frequency of electron hopping in the activated complex may be estimated from $2H_{ab}/h$, the oscillating frequency of the two degenerate diabatic states [16]. Evidently $\nu_{el} \sim 10^{13}$ s^{-1} for interaction energies of only a few hundred cals. A similar estimate is obtained from the Landau-Zener treatment of the intersection region [16]. Since the system typically spends about 10^{-13} s in the intersection region (i.e., $\nu_n \sim 10^{13}$ s^{-1}), the electron transfer will generally be adiabatic for interaction energies larger than about 100 - 300 cal (30 - 100 cm^{-1}).

C. Reorganization Parameters

The reorganization parameter is usually broken down into inner-shell (vibrational) and outer-shell (solvational) components.

$$\lambda = \lambda_{in} + \lambda_{out} \tag{3.5}$$

The inner-shell reorganization energy is generally treated within an harmonic approximation [18]. The outer-shell reorganization energy depends upon the properties of the solvent. When a continuum model for the solvent is used λ_{out} is a function of the dielectric properties of the medium, the distance separating the donor and acceptor sites, and the shape of the reactants.

1. Inner-Shell Reorganization Energy

In order to illustrate the approach used to calculate the inner-shell comtribution to the reorganization barrier we consider the symmetrical stretching vibrations of the two reactants in the $Fe(H_2O)_6^{2+}$ - $Fe(H_2O)_6^{3+}$ self-exchange reaction (Eq. (2.1a)). The inner-shell reorganization term is the sum of the reorganization parameters of the individual reactants, i.e.,

$$\lambda_{in} = \lambda_2(d_2^0 \rightarrow d_3^0) + \lambda_3(d_3^0 \rightarrow d_2^0) \tag{3.6a}$$

The first term on the RHS is the energy required to change the Fe-O distance in $Fe(H_2O)_6^{2+}$ from its equilibrium value d_2^0 to the equilibrium value d_3^0 in $Fe(H_2O)_6^{3+}$ and the second term is the energy required to change the Fe-O distance in $Fe(H_2O)_6^{3+}$ from d_3^0 to d_2^0. Denoting $(d_2^0 - d_3^0)$ by Δd^0, the vertical reorganization energy is given by Eqs. (3.6b) and (3.6c) where f_2 and f_3 are the respective breathing force constants.

$$\lambda_{in} = \frac{6f_2(\Delta d^0)^2}{2} + \frac{6f_3(\Delta d^0)^2}{2} \tag{3.6b}$$

$$= 3(f_2 + f_3)(\Delta d^0)^2 \tag{3.6c}$$

Evidently the contributions of the $Fe(H_2O)_6^{2+}$ and $Fe(H_2O)_6^{3+}$ breathing modes to λ_{in} are *directly* proportional to their respective force constants.

In the activation process, the energy required to reach the transition state configuration is given by

$$\Delta G_m^{\ddagger} = 3f_2(d_2^0 - d_2^{\ddagger})^2 + 3f_3(d_3^0 - d_3^{\ddagger})^2 \tag{3.7a}$$

Energy conservation requires that the Fe-O distances in the $Fe(H_2O)_6^{2+}$ and $Fe(H_2O)_6^{3+}$ adjust to a common value d^* prior to the electron transfer.

$$d_2^* = d_3^* = d^* \tag{3.7b}$$

Minimizing the resulting reorganization energy expression yields Eq. (3.7c) and substitution into Eq. (3.7a) gives Eq. (3.7d).

$$d^* = \frac{f_2 d_2^0 + f_3 d_3^0}{f_2 + f_3} \tag{3.7c}$$

$$\Delta G_{in}^* = \frac{3 f_2 f_3 \left(\Delta d^0\right)^2}{f_2 + f_3} \tag{3.7d}$$

$$\left(d_2^0 - d^*\right) = \frac{f_3 \Delta d^0}{f_2 + f_3} \tag{3.7e}$$

$$\left(d^* - d_3^0\right) = \frac{f_2 \Delta d^0}{f_2 + f_3} \tag{3.7f}$$

The ratio of the amounts that the $Fe(H_2O)_6^{2+}$ and $Fe(H_2O)_6^{3+}$ ions reorganize is equal to f_3/f_2 *i.e.*, *inversely* proportional to their force constants. Since f_3 is larger than f_2, the $Fe(H_2O)_6^{2+}$ ion reorganizes more than the $Fe(H_2O)_6^{3+}$ ion. Note also that $\Delta G_{in}^* < \lambda_{in}/4$ because the free-energy surfaces are not harmonic along the reaction coordinate [15].

Considerable simplification results from using a common, reduced value f_{in} for the force constant of the $Fe(H_2O)_6^{2+}$ and $Fe(H_2O)_6^{3+}$ symmetrical stretching vibrations.

$$f_{in} = \frac{2 f_2 f_3}{\left(f_2 + f_3\right)} \tag{3.8}$$

Under these conditions

$$d^* = \frac{\left(d_2^0 + d_3^0\right)}{2} \tag{3.9a}$$

$$\Delta G_{in}^* = \frac{3 f_{in} \left(\Delta d^0\right)^2}{2} \tag{3.9b}$$

$$\lambda_{in}^s = 6 f_{in} \left(\Delta d^0\right)^2 \tag{3.9c}$$

and the two symmetrized reactants reorganize to the same extent with ΔG_{in}^* now equal to $\lambda_{in}/4$.

The relationship between the vertical reorganization parameter and the activation energy and the effect of using differ criteria for the inner-shell reorganization have recently been considered in some detail [15]. The reorganization energy and the contributions of the individual reactants turn out to be quite sensitive to the model used.

2. Solvent Reorganization Energy

Because of Coulomb interaction terms the solvent reorganization energy is not as readily broken down into contributions from the separate reactants. We illustrate the approach used to calculate the solvent reorganization energy by using the zero-electronic-interaction, two-sphere model developed by Marcus [1, 19, 20].

The familiar Born expression for the free energy of equilibrium solvation of a charged sphere is

$$\Delta G_{eq} = -\frac{(qe)^2}{2a}\left[1-\frac{1}{D_s}\right] \tag{3.10}$$

where qe is the charge on the ion, a is its radius and D_S is the static dielectric constant of the medium. The equilibrium solvation energy can be resolved into two contributions

$$\Delta G_{eq} = -\frac{(qe)^2}{2a}\left[1-\frac{1}{D_{op}}\right]-\frac{(qe)^2}{2a}\left[\frac{1}{D_{op}}-\frac{1}{D_s}\right] \tag{3.11}$$

where the first contribution is the equilibrium solvation due to the electronic polarization of the medium and the second is the contribution from its orientational-vibrational polarization. D_{op} is the optical dielectric constant of the medium. Note that the orientational-vibrational polarization term contains the Pekar factor $(1/D_{op} - 1/D_S)$. The electronic polarization is assumed to be rapid and capable of keeping up with the transferring electron. The orientational-vibrational polarization is much slower and lags behind. Energy conservation requires that the orientation-vibrational polarization adjust to a nonequilibrium value prior to the electron transfer.

Marcus devised a two-step path for calculating the reversible work required to establish a nonequilibrium orientational-vibrational polarization of the medium. In the first step the orientational-vibrational and electronic polarization of the medium is changed from being in

equilibrium with the initial charges q_2^0 and q_3^0 to being in equilibrium with the (hypothetical) charges q_2^* and q_3^*. In the second step the orientational-vibrational polarization remains appropriate to q_2^* and q_3^* but the electronic polarization is changed back to being in equilibrium with q_2^0 and q_3^0. The energy required to reorganize the solvent to the nonequilibrium configuration appropriate to charges q_2^* and q_3^* is then the sum of the work done in these two paths.

$$\Delta G_{out}^{\ddagger} = e^2\left(\frac{\left[q_2^* - q_2^0\right]^2}{2a} + \frac{\left[q_3^* - q_3^0\right]^2}{2a} + \frac{\left(q_2^* - q_2^0\right)\left(q_3^* - q_3^0\right)}{r}\right)\left(\frac{1}{D_{op}} - \frac{1}{D_s}\right) \tag{3.12}$$

The reactants are treated as rigid spheres and their radii are not allowed to change during the reorganization process: the radii in Eq. (3.12) are the average radii defined by $1/a = (1/a_2 + 1/a_3)/2$ and r is the distance between the centers of the spheres. *Note that the numerators in Eq. (3.12) contain the square of the difference of the charges (or, in the case of the electrostatic interaction term, the product of charge differences) and are not simply differences between the squares of charges, as might have been expected on the basis of the Born equation.*

Analogous to the case of the inner-shell reorganization, energy conservation requires that the transition-state charges for the solvent reorganization be equal.

$$q_2^* = q_3^* = q^* \tag{3.13a}$$

Minimizing the resulting solvent reorganization expression yields

$$q^* = (q_2^0 + q_3^0)/2 \tag{3.13b}$$

and substitution into Eq. (3.12) yields Eq. (3.14a) for the free energy of activation

$$\Delta G_{out}^{\ddagger} = \frac{e^2}{4}\left(\frac{1}{2a_2} + \frac{1}{2a_3} - \frac{1}{r}\right)\left(\frac{1}{D_{op}} - \frac{1}{D_s}\right) \tag{3.14a}$$

where it has been assumed that the zero-interaction donor and acceptor sites differ by a single electron, i.e., $(q_3^0 - q_2^0) = 1$. Similarly, substitution into Eq. (3.12) of $q_2^* = q_3^0$ and $q_3^* = q_2^0$ yields Eq. (3.14b) for the solvent reorganization energy in a vertical one-electron transition with $\lambda_{out} = 4\Delta G_{out}^*$.

$$\lambda_{out} = e^2\left(\frac{1}{2a_2} + \frac{1}{2a_3} - \frac{1}{r}\right)\left(\frac{1}{D_{op}} - \frac{1}{D_s}\right) \tag{3.14b}$$

If there is appreciable delocalization in the initial (equilibrium) state then less than a unit of charge will be transferred from the donor to the acceptor. In terms of the mixing coefficients the zero-interaction charge difference $(q_2^0 - q_3^0)$ needs to be scaled by $(c_a^2 - c_b^2)_{eq} = (1 - 2c_b^2)_{eq}$ to obtain the "real" charge transferred. We thus obtain

$$\Delta q = (c_a^2 - c_b^2)_{eq} = (1 - 2c_b^2)_{eq} \tag{3.15}$$

At the minimum of the adiabatic curve, i.e., at the equilibrium configuration of the reactants, $(c_b^2)_{eq}$ is given by Eq. (2.17) so that

$$\left[\left(1 - 2c_b^2\right)_{eq}\right]^2 = \left(1 - \frac{4H_{ab}^2}{\lambda^2}\right) \tag{3.16}$$

Electron delocalization in the initial state thus scales the solvent activation barrier by $(1 - 4H_{ab}^2/\lambda^2)$.

The vertical reorganization parameter λ is a property of the diabatic states, ($H_{ab} = 0$) and λ_{out} continues to be given by Eq. (3.14b) *regardless of the degree of initial state delocalization.* When appreciable delocalization is present we add a prime to indicate that λ has been modified to allow for the reduction in the charge transferred [15, 21]. In other words, λ' denotes a reorganization energy that has been scaled by $(1 - 4H_{ab}^2/\lambda^2)$. (The parameter λ' used here and in [15] corresponds to λ_{mod} introduced earlier [21].)

$$\lambda'_{out} = \lambda_{out}\left(1 - \frac{4H_{ab}^2}{\lambda^2}\right) \tag{3.17a}$$

Similar considerations apply to the inner-shell reorganization. When initial-state delocalization is present $(d_2^0 - d_3^0)$ is scaled by $(1 - 2c_b^2)_{eq}$ giving

$$\lambda'_{in} = \lambda_{in}\left(1 - \frac{4H_{ab}^2}{\lambda^2}\right) \tag{3.17b}$$

Consequently

$$\lambda' = \lambda'_{in} + \lambda'_{out} = \lambda\left(1 - \frac{4H_{ab}^2}{\lambda^2}\right) \qquad (3.17c)$$

In a sense the primed (scaled) quantities are the "actual" vertical reorganization energies since their values are determined by the actual charge transferred. While it would be convenient if λ' was the seperation between the diabatic energy curves at the reactant's equilibrium configuration (X_{min}), it is not. The diabatic curves (H_{ab} =0) correspond to a charge transfer of one electron with this charge abruptly transferring at the transition state: delocalization is *not* incorporated into the diabatic surfaces. This topic is discussed further under optical charge transfer in Section IIID.

3. Time Scales for Solvent Electronic Polarization and Electron Transfer

The above treatment is based upon the traditional Born-Oppenheimer approximation which states that, when nuclei move, the electrons can almost instantaneously adjust to their new positions. Another relevant time frame is the time required to establish the electronic polarization of the medium. In order to characterize this time frame Kim and Hynes consider the ratio of ν_{el}, the electron hopping frequency, to ν_{ep}, the frequency characteristic of the solvent electronic polarization. The Born-Oppenheimer-based treatment is valid provided that this ratio is much less than unity, i.e., the time scale for the adjustment of the electronic polarization is much shorter than that for the transferring electron [22-26].

The electron hopping frequency may be estimated from time-dependent perturbation theory. If H_{ab} is treated as a constant perturbation, the system will start to oscillate between the two diabatic states once the perturbation is turned on. In a bimolecular reaction, for example, the perturbation is turned on upon formation of the precursor complex, while in a covalently attached (bridged) binuclear system it can be turned on upon reduction (oxidation) of one end of the fully oxidized (reduced) system by an external reagent or by photoexcitation. If the system is in the diabatic reactant state at $t = 0$, then the probability of it being in the product state at some later time t is given by the Rabi formula [27].

$$P_2 = \left[\frac{4H_{ab}^2}{(G_2 - G_1)^2}\right]\sin^2\left[\frac{(G_2 - G_1)}{h}\pi t\right] \qquad (3.18)$$

Consider first the case where the system is initially at the nuclear configuration of the adiabatic minimum, i.e., $(G_2 - G_1) = \lambda$. The system will start to oscillate between the two

diabatic states with a frequency equal to λ/h which corresponds to $\sim 5 \times 10^{14}$ s^{-1} for $\lambda = 40$ kcal mol^{-1}. The maximum value of the probability of finding the system in the product state is $4H_{ab}^2/\lambda^2$ or 2×10^{-3} for $H_{ab}/\lambda = 2 \times 10^{-2}$. There is thus only a very small probability that weak coupling will drive the system into the product state at a nuclear configuration near the initial state minimum. Since the frequency with which the system oscillates under the influence of the perturbation is λ/h, the maximum frequency of attaining the product state (*i.e.*, the maximum probablity per unit time) is $4H_{ab}^2/h\lambda$. In other words, ν_{el} at the adiabatic minimum is estimated to be $\approx 10^{12}$ s^{-1} for a moderately coupled Class II system ($H_{ab} \approx 100$ cm^{-1}, $\lambda \approx 10$ kcal mol^{-1}). Since $\nu_{ep} \sim 10^{15}$ s^{-1} or higher for most colorless solvents [25], the ratio ν_{el}/ν_{ep} is much less than unity for a weakly or moderately coupled Class II system near the adiabatic minmum.

We turn next to the frequency of electron hopping in the transition state. As is evident from Eq. (3.18) with $(G_2 - G_1) = 2H_{ab}$, the frequency of electron hopping in the transition state is equal to $2H_{ab}/h$ (see also the discussion following Eq. (3.4)). Thus the transition-state hopping frequency ν_{el} is $\leq 10^{13}$ s^{-1} for a weakly or moderately coupled Class II system and $\nu_{el}/\nu_{ep} << 1$ at the transition state. Thus the condition for the validity of the Born-Oppenheimer approximation will be satisfied by most weakly and moderately coupled Class II systems. For symmetrical Class II systems the free energy of activation will then be given by the traditional Eq. (2.14) [22-26] except that a correction for the so-called exchange field may be needed under certain circumstances. The exchange field arises from the overlap charge distribution ($e\psi_a\psi_b$) and serves to lower λ_{out} (more correctly, to stabilize the transition state) and to reduce the effective H_{ab} [22, 25]. However, there is no exchange field when the diabatic wave functions are appropriately chosen, i.e., when they are based on the exchange dipole moment (μ_{ab}, see below) being zero [28] and no exchange-field correction to the traditional expression for the free energy of activation is then required.

In the Born-Oppenheimer limit the electrons of the surrounding medium equilibrate to the instantaneous position of the transferring electron while the orientations of the medium dipoles, which occur much more slowly, adjust to the smeared-out charge distribution of the transferring electron. When the time scale for electronic polarization is slower than, or comparable to, the time scale of the transferring electron, it becomes necessary to use a self-consistent treatment in which both the electronic polarization and the orientational polarization respond to the smeared-out charge distribution of the transferring electron [25]. Including the interaction of this charge distribution with the electronic polarization gives rise to a nonlinear Schrodinger equation in which the Hamiltonian depends on the wave function for the donor-acceptor pair. Such a treatment becomes increasingly important as the electronic interaction increases and introduces terms into the free energy of activation that have the net effect of *increasing* the activation energy beyond that given by the Born-Oppenheimer limit [25]. In the limit that the time scale for

the solvent electronic polarization becomes very long the electronic polarization can no longer keep up with the transferring electron and the electronic polarization will contribute to the activation barrier in much the same way as the orientational-vibrational polarization.

D. Optical Charge Transfer

In addition to thermal activation, electron transfer between the donor and acceptor sites can also be effected by the absorption of light. As a consequence, λ and H_{ab} can be obtained from spectroscopic properties.

1. Transition Energies

The energy of the light-induced charge transfer transition in a symmetrical double-well system is given by Eq. (3.19) [29, 30].

$$\nu_{max} = \lambda \tag{3.19}$$

Since λ for a symmetrical localized system is *independent* of H_{ab}, Eq. (3.19) holds throughout the double well regime [11]. Further insight into Eq. (3.19) can be obtained by noting that ν_{max} is also given by

$$\nu_{max} = \lambda' + 4H_{ab}^2/\lambda \tag{3.20}$$

The first term on the RHS is the scaled reorganization energy and the second term is a further quantum-mechanical contribution to the transition energy. Although the scaled reorganization energy associated with the charge transfer is reduced by the delocalization, this decrease is compensated for by the repulsion of the curves. The net effect is that ν_{max} remains constant. Thus, even when appreciable delocalization is present, ν_{max} will still exhibit the full solvent dependence predicted for the very weakly interacting system.

The energy of the optical transition in a symmetrical Class III system is given by

$$\nu_{max} = 2H_{ab} \tag{3.21}$$

so that H_{ab} for symmetrical Class III complexes can be obtained directly from the energy of the optical transition [29]. Note that the optical transition in a Class III system no longer involves charge transfer: the transition occurs between delocalized molecular orbitals of the complex and is not accompanied by a net dipole-moment change.

The energy of the charge transfer transition in an unsymmetrical double-well system is given by

$$\nu_{max,a} = \left(\lambda + \Delta G^o\right)\left[1 + \frac{2H_{ab}{}^2 \Delta G^o}{(\lambda + \Delta G^o)^3}\right] \tag{3.22}$$

provided that $H_{ab} < (\lambda + \Delta G^o)/2$ [15]. When the $H_{ab}{}^2$ contribution may be neglected, the energy of the charge transfer transition in an unsymmetrical double-well system is given by the familiar Eq. (3.23)

$$\nu_{max,a} = \lambda + \Delta G^o \tag{3.23}$$

Finally, although ν_{max} for a symmetrical double well system is independent of the degree of electronic interaction, the free energy of activation does depend on H_{ab}. Thus when ΔG^o may be neglected, the ratio $\nu_{max}/\Delta G^*$ for a double-well system is given by

$$\frac{\nu_{max,a}}{\Delta G^*} = \frac{4}{\left(1 - 2H_{ab}/\lambda\right)^2} \tag{3.24a}$$

while, when the electronic interaction may be neglected, the ratio is given by

$$\frac{\upsilon_{max,a}}{\Delta G^*} = \frac{4}{1 + \Delta G^0/\lambda} \tag{3.24b}$$

Evidently $\nu_{max}/\Delta G^*$ is ≤ 4 for a weakly coupled, endergonic charge-transfer reaction and ≥ 4 for a weakly coupled, exergonic charge-transfer reaction or for charge transfer in a moderately coupled symmetrical double-well system. The value of $\nu_{max}/\Delta G^*$ can thus provide information about the degree of electronic interaction. However, in practice the latter is more readily obtained from the intensity of the charge transfer transition.

2. Intensities and Dipole-Moment Changes

Using the Mulliken formalism, Hush[29] showed that the electronic coupling element is related to the intensity of the charge transfer transition by

$$H_{ab} = 2.06\times10^{-2}\,\frac{\left(\nu_{max}\varepsilon_{max}\Delta\nu_{1/2}\right)^{1/2}}{r_{ab}} \tag{3.25}$$

where ν_{max} and $\Delta\nu_{1/2}$ are the band maximum and width in wave numbers, r_{ab} is the distance separating the donor and acceptor charge centroids in Ångströms, and the band is Gaussian shaped [11]. *Equation (3.25) is exact within a two-state model and is applicable to both symmetrical and unsymmetrical Class II and Class III systems* [11].

The Mulliken-Hush expression is a particular form of the more general equation

$$H_{ab} = \left|\frac{\nu_{max}\mu_{12}}{\mu_b - \mu_a}\right| \tag{3.26}$$

where μ_{12} is the transition dipole moment and $(\mu_b - \mu_a)$ is the difference between the dipole moments of the initial and final diabatic (localized) states [11, 31]. In the generalized Mulliken-Hush treatment formulated by Cave and Newton [32, 33], the diabatic states are obtained by applying the transformation that diagonalizes the adiabatic dipole moment matrix. Since μ_{ab}, the transition moment connecting the diabatic states, is zero, the value of $(\mu_b - \mu_a)$ is maximized. With this definition of the diabatic states, the diabatic dipole-moment difference is related to the measured dipole-moment change $(\mu_2 - \mu_1)$ by Eq. (3.27). The diabatic dipole-moment difference can thus be obtained from measurable quantities [32].

$$\mu_b - \mu_a = \left[\left(\mu_2 - \mu_1\right)^2 + 4\mu_{12}^2\right]^{1/2} \tag{3.27}$$

Equation (3.25) follows from Eq. (3.26) by noting that $r_{ab} \equiv |(\mu_b - \mu_a)/e|$ and that the transition dipole moment is given by Eq. (3.28)

$$\mu_{12} = \sqrt{\frac{f_{os}}{1.08\times10^{-5}\nu_{max}}} \tag{3.28a}$$

$$f_{os} = 4.61\times10^{-9}\left(\varepsilon_{max}\Delta\nu_{1/2}\right) \tag{3.28b}$$

where f_{os} is the oscillator strength of the transition [11, 31]. Equation (3.21) is obtained by noting that $(\mu_2 - \mu_1)$ is zero for a delocalized system and therefore, from Eq. (3.27), $(\mu_b - \mu_a) = 2\mu_{12}$. Finally, since the adiabatic and diabatic dipole-moment changes are related by

$$(\mu_2 - \mu_1) = (\mu_b - \mu_a)(1 - 2c_b^2) \tag{3.29}$$

it follows from Eq. (2.11c) that

$$\frac{\mu_2 - \mu_1}{\mu_b - \mu_a} = \frac{G_b - G_a}{G_2 - G_1} \tag{3.30}$$

There is thus an inverse relationship between the ratio of the adiabatic and diabatic dipole-moment changes and the ratio of the corresponding free-energy differences within the two-state model.

IV. QUANTUM MECHANICAL TREATMENT

Although the semiclassical expressions work well at high temperatures, they break down at low temperatures and/or at high reaction exergonicities. Nuclear tunneling contributions to the rate can become very important under such conditions. Although corrections for nuclear tunneling can be introduced into the semiclassical treatment, tunneling enters naturally into a quantum mechanical treatment.

The quantum mechanical treatment of nonadiabatic electron transfers are normally considered in terms of the formalism developed for multiphonon radiationless transitions. This formalism starts from Fermi's golden rule for the probability of a transition from an vibronic state A_v of the reactant (electronic state A with vibrational level v) to a vibronic state B_w of the product.

$$W_{A_v} = \frac{4\pi^2 H_{ab}^2}{h}\rho_w \tag{4.1a}$$

$$\rho_w = \sum_w \left|\left\langle \chi_{A_v} \middle| \chi_{B_w} \right\rangle\right|^2 \delta\left(\varepsilon_{A_v} - \varepsilon_{B_w}\right) \tag{4.1b}$$

where ρ_w is the weighted density of final states, ε_{A_v} and ε_{B_w} are the unperturbed energies of the vibronic levels and δ is the delta function that ensures energy conservation. To obtain the thermally averaged probability per unit time, k, of passing from a set of vibrational levels $\{A_v\}$ of the reactant to a set of vibrational levels $\{B_w\}$ of the products we assume a Boltzmann distribution over the vibrational levels of the reactants and sum over these levels.

$$k = \frac{4\pi^2 H_{ab}^2}{h}\left(FC\right) \tag{4.2a}$$

$$FC = \frac{1}{Q}\sum_v \sum_w \exp\left(\frac{-\varepsilon_{A_v}}{RT}\right) S_{A_v,B_w}^2 \delta\left(\varepsilon_{A_v} - \varepsilon_{B_w}\right) \tag{4.2b}$$

$$Q = \sum_v \exp\left(\frac{-\varepsilon_{A_v}}{RT}\right) \tag{4.2c}$$

where FC is the thermally averaged Franck-Condon factor. If the reactant and product energy surfaces are approximated as harmonic, the FC factors can be explicitly calculated [34, 35] .

Three broad classes of vibrational modes need to be considered: the high-frequency (fast) modes ($h\nu > 1000$ cm^{-1}) which are mainly intraligand vibrations, intermediate modes (1000 cm^{-1} $> h\nu >$ 100 cm^{-1}) that typically include the metal-ligand stretching vibrations and higher frequency solvent orientational-vibrational modes, and the low-frequency (slow) modes ($h\nu <$ 100 cm^{-1}) which are primary solvent modes but can include low-frequency intramolecular modes.

At ordinary temperatures $h\nu_V >> kT \sim h\nu_C >> h\nu_S$ and the low-frequency modes can be treated using classical (continuum) expressions.

A. Two-Mode Systems

We first consider the case with one high-frequency mode and one low-frequency mode. When the high-frequency mode (ν_V, with reorganization energy of λ_V) is in the low temperature limit and the low-frequency mode (ν_S, λ_S) is treated classically, the rate constant for electron transfer is given by

$$k_{el} = \frac{H_{ab}^2}{h}\left(\frac{4\pi^3}{\lambda_s RT}\right)^{1/2}\sum_{j=0}^{\infty} F_j \exp\left[-\frac{\left(jh\nu_v + \Delta G^0 + \lambda_s\right)^2}{4\lambda_s RT}\right] \qquad (4.3)$$

where $F_j = \frac{e^{-S}S^j}{j!}$, $S = \frac{\lambda_v}{h\nu_v}$ and $F_j H_{ab}^2 < h\nu_s\sqrt{\frac{\lambda_s RT}{\pi^3}}$ [36-38]. Since the solvent (or other low-frequency) mode behaves classically while the high-frequency mode can tunnel it is most efficient for the solvent modes to use enough of the driving force to reduce the solvent barrier significantly with the remaining driving force absorbed by the high-frequency modes. Moreover, since $h\nu_V >> kT$ all of the reaction occurs from the lowest vibrational level of the initial state, i.e., only $A_0 \rightarrow \{B_j\}$ vibronic transitions are considered. The exponential term in Eq. (4.3) is a Gaussian that describes the rate constant reduction deriving from the solvent reorganization. The Gaussian is peaked at $(jh\nu + \Delta G^0 + \lambda_S) \approx 0$ and has a width of $2\sqrt{4\lambda_s RT}$. The transition with $j^* \approx -(\Delta G^0 + \lambda_S)/h\nu$ will normally dominate the sum. The rate constant will be maximized when the solvent reorganization is barrierless. This occurs when the effective driving force for the solvent reorganization, $-(\Delta G^0 + jh\nu_V)$ is approximally equal to λ_S, i.e., when $j^* \approx -(\Delta G^0 + \lambda_S)/h\nu_V$. The effective energy gap for the high-frequency mode is $-(\Delta G^0 + \lambda_S)$. The energy change of the reactant/product and the solvent for the single largest term in the sum of Eq. (4.3) is plotted vs driving force is illustrated in Figure 7. The solvent accepts an amount of energy that is close to the λ_S for the system while the high-frequency mode will accept no energy for very low driving forces and the majority of the energy change when $|\Delta G^0| >> \lambda_S + \lambda_V$.

A convenient closed-form expression for the rate can be derived using Eq. (4.3).

$$k_{el} = \frac{4\pi^2 H_{ab}^2 F_{j^*}}{h^2 \nu_v}\exp\left[-\frac{\left(j^* h\nu_v + \Delta G^0 + \lambda_s\right)^2}{4\lambda_s RT}\right] \qquad (4.4a)$$

where

$$j^* \approx -\frac{\left(\Delta G^0 + \lambda_s\right)}{h\nu_v} - \frac{2\lambda_s RT(\gamma + 1)}{\left(h\nu_v\right)^2} \qquad (4.4b)$$

$$\gamma = \ln\left[-\frac{\left(\Delta G^0 + \lambda_s\right)}{\lambda_v}\right] - 1 \tag{4.4c}$$

The rate constants in the inverted region calculated from Eq. (4.1) are almost independent of temperature and decrease much less rapidly with driving force than predicted by classical models [39].

B. Three-Mode Systems

Next we consider a reaction that contains an active mode in each of the regions outlined above. The expression for the three-mode case is

$$k_{el} = \frac{H_{ab}^2}{h}\left(\frac{4\pi^3}{\lambda_s RT}\right)^{1/2} \exp\left[-S_c \coth\left(\frac{h\nu_c}{2kT}\right)\right] \sum_{j_v=0}^{\infty}\sum_{j_c=-\infty}^{\infty} F_{f_v} \exp\left(\frac{j_c h\nu_c}{2kT}\right) I_{j_c}\left(S_c \operatorname{csch}\left(\frac{h\nu_c}{2kT}\right)\right) \times \exp\left[-\frac{\left(\Delta G^0 + \lambda_s + j_v h\nu_v + j_c h\nu_c\right)^2}{4\lambda_s RT}\right] \tag{4.5}$$

where j_v and j_c are the changes in the vibrational quantum numbers for the high and intermediate frequency modes, respectively[39]. Again the last exponential term in Eq (4.5) is Gaussian peaked at $\left(\Delta G^0 + \lambda_s + j_v h\nu_v + j_c h\nu_c\right) = 0$ with a width of $2\sqrt{4\lambda_s RT}$. In this case energy sharing can take place between the high-, intermediate- and low-frequency modes; the possibility of energy borrowing is increased but again the low-frequency mode is required to pass over its barrier while the other two modes can tunnel. Figures 8 and 9 show the energy distribution for the dominant contribution to the double sum. The low-frequency mode receives $\approx \lambda_S$ of energy to minimize its barrier; the intermediate mode receives $\approx \lambda_C$, and the bulk of the energy for large driving forces is deposited in the high-frequency mode. Only very seldom is the low or intermediate-frequency energy of the product less than that of the reactant. This is shown in Figure 9 where $\Delta\varepsilon_S$ is negative.

These expressions show that normally most of the excess energy is acquired by the high-frequency mode and that the intermediate-frequency mode receives an amount of energy that is less than one high-frequency vibrational quantum. Only when $\lambda_C >> \lambda_S$ does the intermediate-frequency mode receive significantly more than a single high-frequency quantum. The effect of an intermediate mode on the rate constant for the reaction is relatively modest in the normal region but becomes important in the inverted region where the initial state needs to dispose of significantly more energy (Figure 10). In this region systems that have both high- and intermediate-frequency modes exhibit significant rate enhancements due to tunneling and the decrease of the rate constant with increasing driving force is attenuated. Also, due to the

intermediate-frequency mode the sinusoidal quantum beat effect observed for the dependence of the rate constant von driving force in the inverted region is significantly attenuated.

The three-mode expression is most useful when discussing the rates of nonradiative deactivation of excited states in the inverted region. In this region, where $-\Delta G^0 >> \lambda_v + \lambda_c + \lambda_s$, a much simpler expression can be used since the product is created with a high vibrational quantum number in the high-frequency mode. This expression is Eq (4.6) provided that $5\lambda_c$ and $10\lambda_s$ are each $< |\Delta G^0|$.

$$k_{el} = \frac{4H_{ab}^2}{h}\left[-\frac{\pi^3}{2h\nu_v\left(\Delta G^0 + \lambda_c + \lambda_s\right)}\right]^{1/2} \times \exp\left(-\frac{\lambda_v - (\gamma_0+1)(\lambda_c+\lambda_s) - \gamma_0\Delta G^0 - \frac{(\gamma_0+1)^2}{h\nu_v}\left(\lambda_s RT + \frac{\lambda_c h\nu_c}{2}\coth\left(\frac{h\nu_c}{2kT}\right)\right)}{h\nu_v}\right) \quad (4.6a)$$

where

$$\gamma_0 = \ln\left(\frac{-\Delta G^0}{\lambda_v}\right) - 1 \quad (4.6b)$$

The above three-mode expression very well approximates the more exact expression Eq. (4.5) but does not show the quantum beat effect.

V. CONCLUSIONS

The expressions derived from the traditional two-state model are useful in rationalizing a variety of electron transfer processes. Both thermal and optical charge transfer can be treated and, although not discussed here, electrochemical processes as well. The two-state model neglects contributions from higher electronic states in calculating the energies of the zero-order ground states of the reactants and products. Contributions from higher electronic states are, however, frequently needed in calculating electronic coupling elements. Mixing with such states leads to modification of the ground-state energies when the excited states are sufficiently low lying. Such perturbations are absent in the zero-interaction limit.

Some key features of the two-state model are summarized here:

(1) Although the reaction coordinate for charge transfer is not uniquely defined, the vertical difference between the zero-order reactant and product free energies is related to the degree of nuclear reorganization and consequently this difference provides a useful measure of the progress of the reaction(Section IIA).

(2) The degree of charge transfer is *not* linearly related to the reaction coordinate defined above (Section IIB).

(3) The splitting at the intersection of the adiabatic curves for a self-exchange reaction, $2H_{ab}$, enters into the expression for the free energy of activation for the exchange reaction analogous to the manner in which the driving force, $-\Delta G^{o}$, enters into the expression for the free energy of activation for a marginally adiabatic net reaction (Section IIB).

(4) The vertical difference between the free energies of the reactants and products of a self exchange reaction remains equal to λ at the equilibrium configuration of the reactants (or products) regardless of the magnitude of the electronic coupling as long as the system remains valence trapped (Sections IIB and IIIB).

(5) The frequency of electron hopping in the transition state is equal to $2H_{ab}/h$ (Section IIIC).

(6) The electron transfer distance is defined by the difference between the dipole moments of the localized (diabatic) reactant and product states (Section IIID).

(7) At low temperatures and/or at high reaction exergonicities nuclear tunneling contributions to the rate and other quantum effects become important. Two- and three-mode expressions are presented that allow for tunneling of the higher frequency modes (Section IV).

Overall, the two-state model is remarkably successful in interpreting electron transfer and related properties and forms the cornerstone for interpreting a variety of complex physical, photosynthetic, catalytic and biological processes.

ACKNOWLEDGMENTS

We wish to acknowledge helpful discussions with Rudolph A. Marcus. This research was carried out at Brookhaven National Laboratory under contract DE-AC02-98CH10886 with the U.S. Department of Energy and was supported by its Division of Chemical Sciences, Office of Basic Energy Sciences.

[1] R. A. Marcus, *J. Chem. Phys. 26* (1957) 867-871.

[2] R. A. Marcus, *Disc. Faraday. Soc. 29* (1960) 21-31.

[3] R. A. Marcus, *Rev. Modern Phys. 65* (1993) 599-610.

[4] N. Sutin, *Prog. Inorg. Chem. 30* (1983) 441-498.

[5] R. A. Marcus, N. Sutin, *Biochim. Biophys. Acta 811* (1985) 265-322.

[6] The sum of any two parabolas gives a parabola that has a force constant equal to the sum of the force constants of the two original parabolas and with its minimum located above the two original minima and horizonally between them.

[7] J.-K. Hwang, A. Warshel, *J. Am. Chem. Soc. 109* (1987) 715-720.

[8] G. King, A. Warshel, *J. Chem. Phys. 93* (1990) 8682-8692.

[9] R. A. Marcus, N. Sutin, *Inorg. Chem 14* (1975) 213-216.

[10] L. W. Ungar, M. D. Newton, G. A. Voth, *J. Phys. Chem. B. 103* (1999) 7367-7382.

[11] C. Creutz, M. D. Newton, N. Sutin, *J. Photochem. Photobiol.A: Chem. 82* (1994) 47-59.

[12] M. B. Robin, P. Day, *Adv. Inorg. Chem. Radiochem. 10* (1967) 247-422.

[13] C. Creutz, *Prog. Inorg. Chem. 30* (1983) 1-73.

[14] R. J. Crutchley, *Adv. Inorg. Chem. 41* (1994) 273-325.

[15] B. S. Brunschwig, N. Sutin, *Coord. Chem. Rev. 187* (1999) 233-254.

[16] N. Sutin, in G. L. Gunther (Ed.): *Bioinorganic Chemistry, Vol. 2*, Elsevier, New York 1973, p. 611-653.

[17] B. S. Brunschwig, J. Logan, M. D. Newton, N. Sutin, *J. Am. Chem. Soc. 102* (1980) 5798-5809.

[18] R. A. Marcus, *Ann. Rev. Phys. Chem. 15* (1964) 155-196.

[19] R. A. Marcus, *J. Chem. Phys. 24* (1956) 966-978.

[20] R. A. Marcus, *J. Chem. Phys. 43* (1965) 679-701.

[21] B. S. Brunschwig, C. Creutz, N. Sutin, *Coord. Chem. Rev. 177* (1998) 61-79.

[22] H. J. Kim, J. T. Hynes, *J. Chem. Phys. 93* (1990) 5194-5210.

[23] J. N. Gehlen, D. Chandler, H. J. Kim, J. T. Hynes, *J. Phys. Chem. 96* (1992) 1748-1753.

[24] R. A. Marcus, *J. Phys. Chem. 96* (1992) 1753-1757.

[25] H. J. Kim, J. T. Hynes, *J. Chem. Phys. 96* (1992) 5088-5110.

[26] J. N. Gehlen, D. Chandler, *J. Chem. Phys. 97* (1992) 4958-4963.

[27] P. W. Atkins, *Molecular Quantum Mechanics*, Oxford University Press, New York 1983.

[28] H. J. Kim, R. Bianco, B. J. Gertner, J. T. Hynes, *J. Phys. Chem. 97* (1993) 1723-1728.

[29] N. S. Hush, *Prog. Inorg. Chem. 8* (1967) 391-444.

[30] N. S. Hush, *Electrochim. Acta 13* (1968) 1005-1023.

[31] Y.-g. K. Shin, B. S. Brunschwig, C. Creutz, N. Sutin, *J. Phys. Chem. 100* (1996) 8157-8169.

[32] R. J. Cave, M. D. Newton, *Chem. Phys. Lett. 249* (1996) 15-19.

[33] R. J. Cave, M. D. Newton, *J. Chem. Phys. 106* (1997) 9213-9226.

[34] The overlap integrals $S_{Av,Bw}$ can be calculated if the reactant and produce surfaces are assumed to be harmonic with the same force constants. The overlap inegral is then given by

$$S_{A_v,B_w} = \left(\frac{Z}{\sqrt{2}}\right)^{w-v} L_v^{w-v}\left(z^2/2\right)\exp\left(-\frac{z^2}{4}\right)$$

where $z = \left(\frac{2\lambda}{h\nu}\right)^{1/2}$ and $L_v^{w-v}(z)$ are generalized Laguerre polynomials.

[35] T. Terasaka, T. Matsushita, *Chem. Phys. Let. 80* (1981) 306-310.

[36] J. Ulstrup, J. Jortner, *J. Chem. Phys. 63* (1975) 4358-4368.

[37] J. Jortner, *J. Chem. Phys. 64* (1976) 4860-4867.

[38] J. Ulstrup, *Charge Transfer Processes in Condensed Media*, Springer-Verlag, New York 1979.

[39] B. S. Brunschwig, N. Sutin, *Comments Inorg. Chem. 6* (1987) 209-235.

Figure 1. Plot of the diabatic free-energies of the reactants (left-hand curve, G_a) and products (right-hand curve, G_b) vs the reaction coordinate for an electron transfer reaction with $\Delta G^0 = 0$. The sum (dots) and difference (dot-dash) of the reactant and product free-energies are also plotted.

Figure 2. Plot of the diabatic free-energies of the reactants (G_a) and products (G_b) vs the reaction coordinate for an electron transfer reaction with $\Delta G^0 < 0$. The sum (dots) and difference (dot-dash) of the reactant and product free-energies are also plotted.

Figure 3. Plot of the diabatic (G_a, G_b) and adiabatic (G_1, G_2) free-energies of the reactants and products vs the reaction coordinate for an electron transfer reaction with $\Delta G^0 = 0$. H_{ab} is the electronic coupling element between the diabatic states of the reactants and products and λ is the reorganization energy for the reaction.

Figure 4. Plot of the adiabatic free-energy surfaces vs the reaction coordinate for an electron transfer reaction with $\Delta G^0 = 0$ and H_{ab}/λ varying from 0 to 0.5.

Figure 5. Plot of the differences between the adiabatic free-energy curves shown in Figure 4 vs the reaction coordinate for an electron transfer reaction with $\Delta G^0 = 0$ and H_{ab}/λ varying from 0 to 0.5.

Figure 6. Plot of c_b^2 vs the reaction coordinate using Eq. (2.12) with H_{ab}/λ varying from 0 to 0.5.

Figure 7. Plot of the energy in a particular mode for an electron transfer reaction with two active modes. $\Delta\varepsilon_v$ and $\Delta\varepsilon_s$ are the differences between the energies of the products and reactants in the high- and low-frequency modes, respectively; λ_i, (cm^{-1}) and $h\nu_i$ (cm^{-1}) are (2000, 2000) and (1200, –) for the high- and low-frequency modes and the temperature is 300 K. The calculations were done using Eq. (4.5). The straight line, the stepped solid line and the dotted lines are the total energy difference (ΔG^0) and the differences between the energies of the products and reactants in the high- and low-frequency modes, respectively.

Figure 8. Plot of the energy in a particular mode for an electron transfer reaction with three active modes. $\Delta\varepsilon_v$, $\Delta\varepsilon_c$ and $\Delta\varepsilon_s$ are the differences between the energies of the products and reactantsin the high-, intermediate- and low-frequency modes, respectively; λ_i, (cm^{-1}) and $h\nu_i$ (cm^{-1}) are (2000, 2000); (200, 200); and (1000, –) for the high-, intermediate- and low-frequency modes and the temperature is 300 K. The calculations were done using Eq. (4.5). The straight line, the stepped solid line, the dashed line and the dotted lines are the total energy difference (ΔG^0) and the differences between the energies of the products and reactants in the high-, intermediate- and low-frequency modes, respectively.

Figure 9. Plot of the energy in a particular mode for an electron transfer reaction with three active modes. $\Delta\varepsilon_v$, $\Delta\varepsilon_c$ and $\Delta\varepsilon_s$ are the difference between the energies of the products and reactants in the high-, intermediate- and low-frequency modes λ_i, (cm^{-1}) and $h\nu_i$ (cm^{-1}) are (2000, 2000); (1000, 200); and (200, –) for the high-, intermediate- and low-frequency modes, respectively, and the temperature is 300 K. The calculations were done using Eq. (4.5). The straight line, the stepped solid line, the dashed line and the dotted lines are the total energy difference (ΔG^0) and the differences between the energies of the products and reactants in the high-, intermediate- and low-frequency modes, respectively.

Figure 10. Plot of the logarithm of the Franck-Condon factors for the electron transfer reaction calculated using the classical expression, Eq. (3.3); two-mode expression, Eq. (4.3); three-mode expression, Eq. (4.5); and the approximate three-mode expression, Eq. (4.6) vs driving force. The parameters used (λ_s, λ_c, $h\nu_c$, λ_h, $h\nu_h$ in cm^{-1}) for the calculations are classical: (3200); two-mode, (1200, 2000, 600); three-mode (600, 600, 200, 2000, 600) and the temperature is 80 K. The solid line (inverted parabola), dotted line, oscillating solid line and the dashed line are for the classical expression, Eq. (3.3), the two-mode expression, Eq. (4.3), the full three-mode expression, Eq. (4.5), and the approximate three-mode expression, Eq. (4.6), respectively.

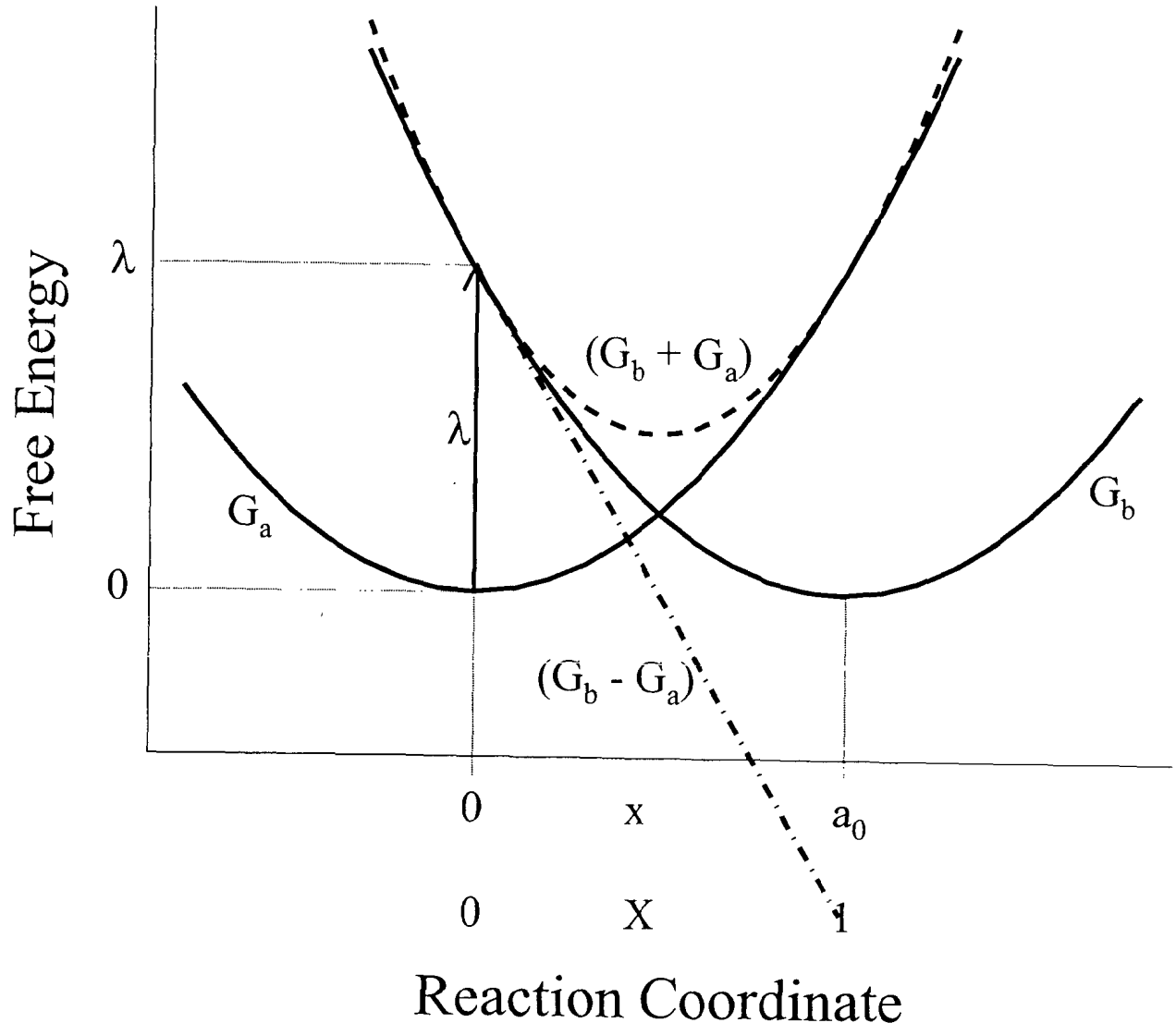
Free Energy
λ
0
$(G_b + G_a)$
λ
G_a
G_b
$(G_b - G_a)$
0
x
a_0
0
X
1
Reaction Coordinate

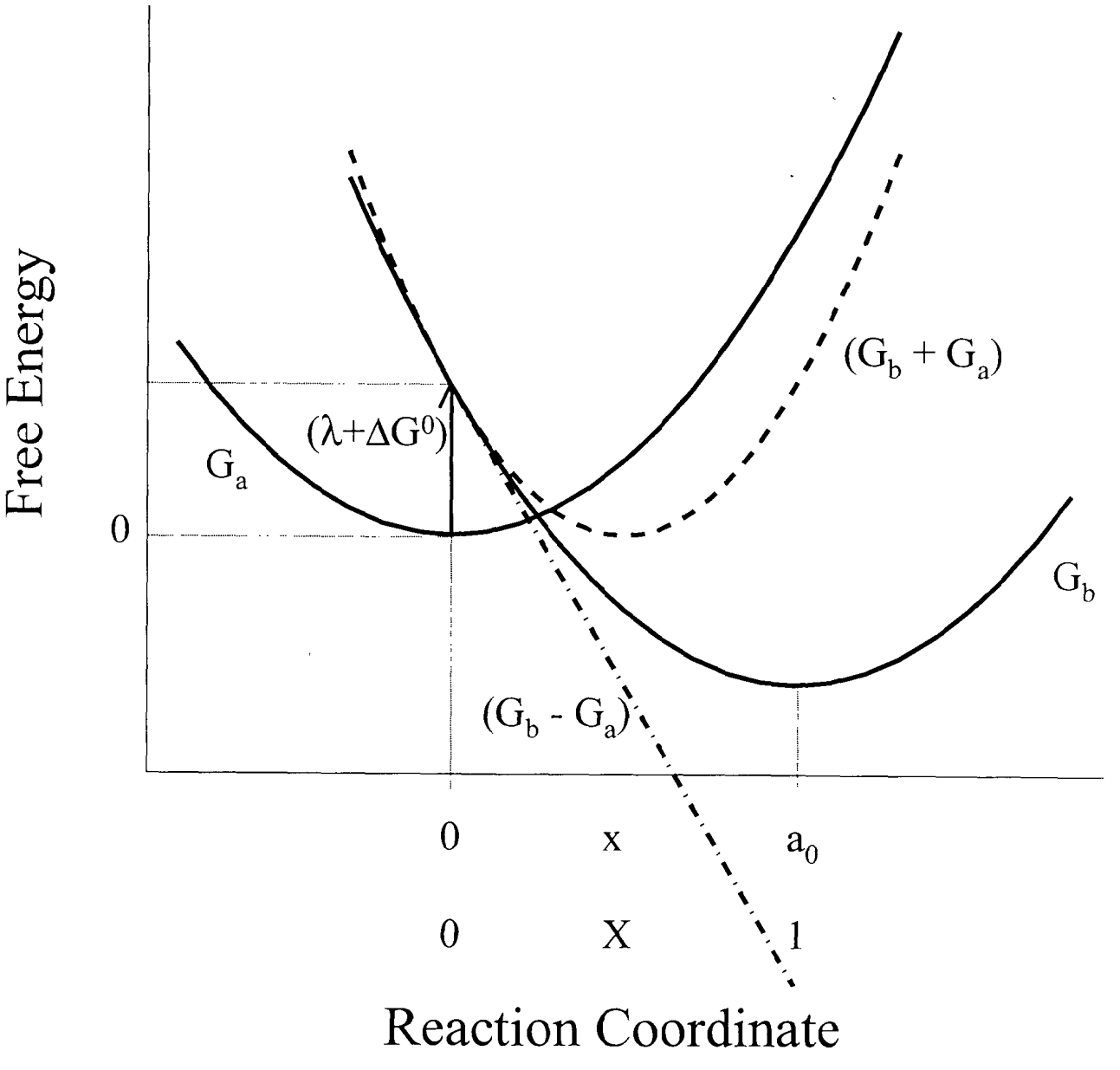
Free Energy
0
G_a
$(\lambda+\Delta G^0)$
$(G_b + G_a)$
G_b
$(G_b - G_a)$
0
x
a_0
0
X
1
Reaction Coordinate

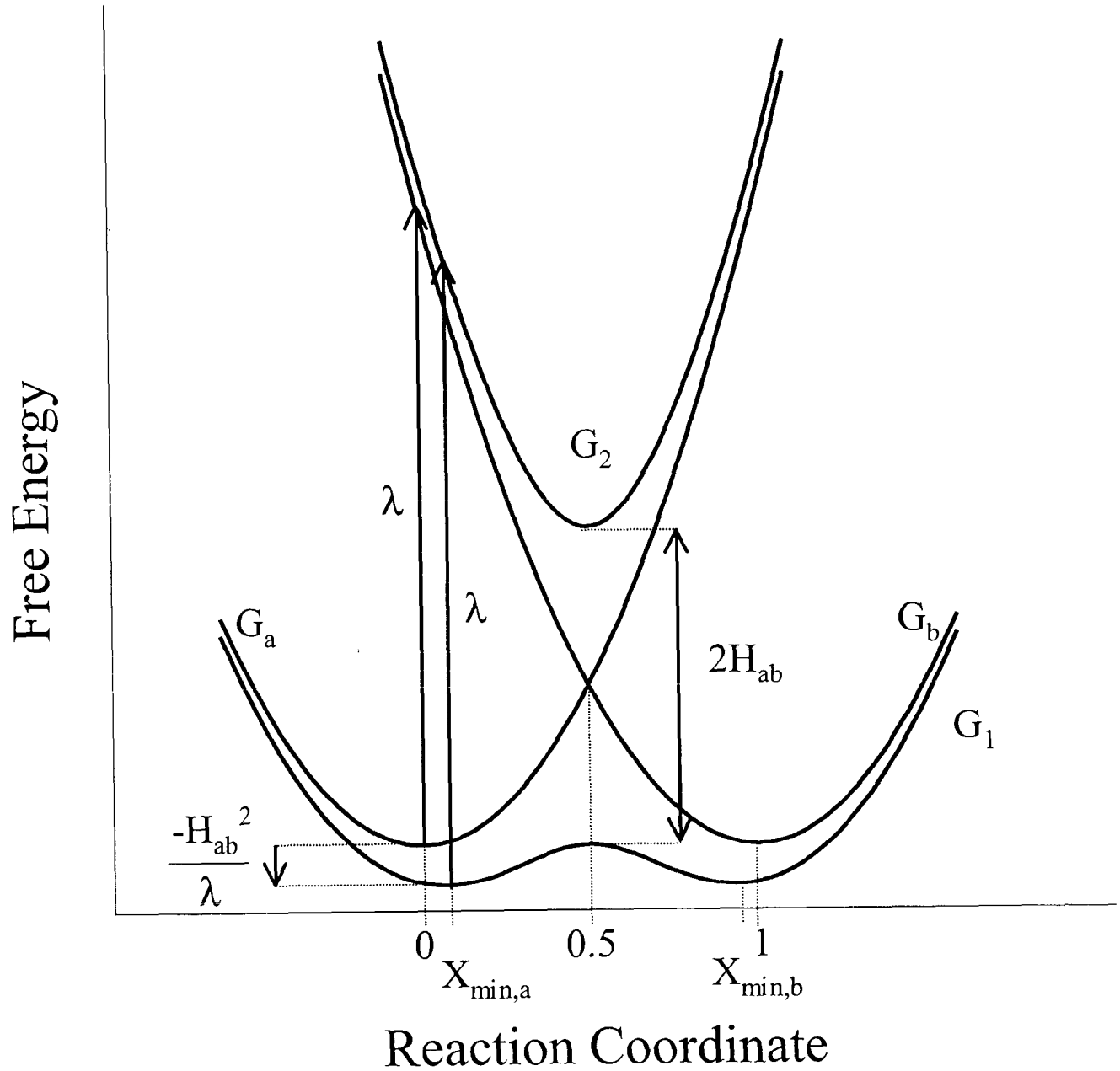
Free Energy
G_2
λ
λ
G_a
G_b
$2H_{ab}$
G_1
$\frac{-H_{ab}^2}{\lambda}$
0
0.5
1
$X_{min,a}$
$X_{min,b}$
Reaction Coordinate

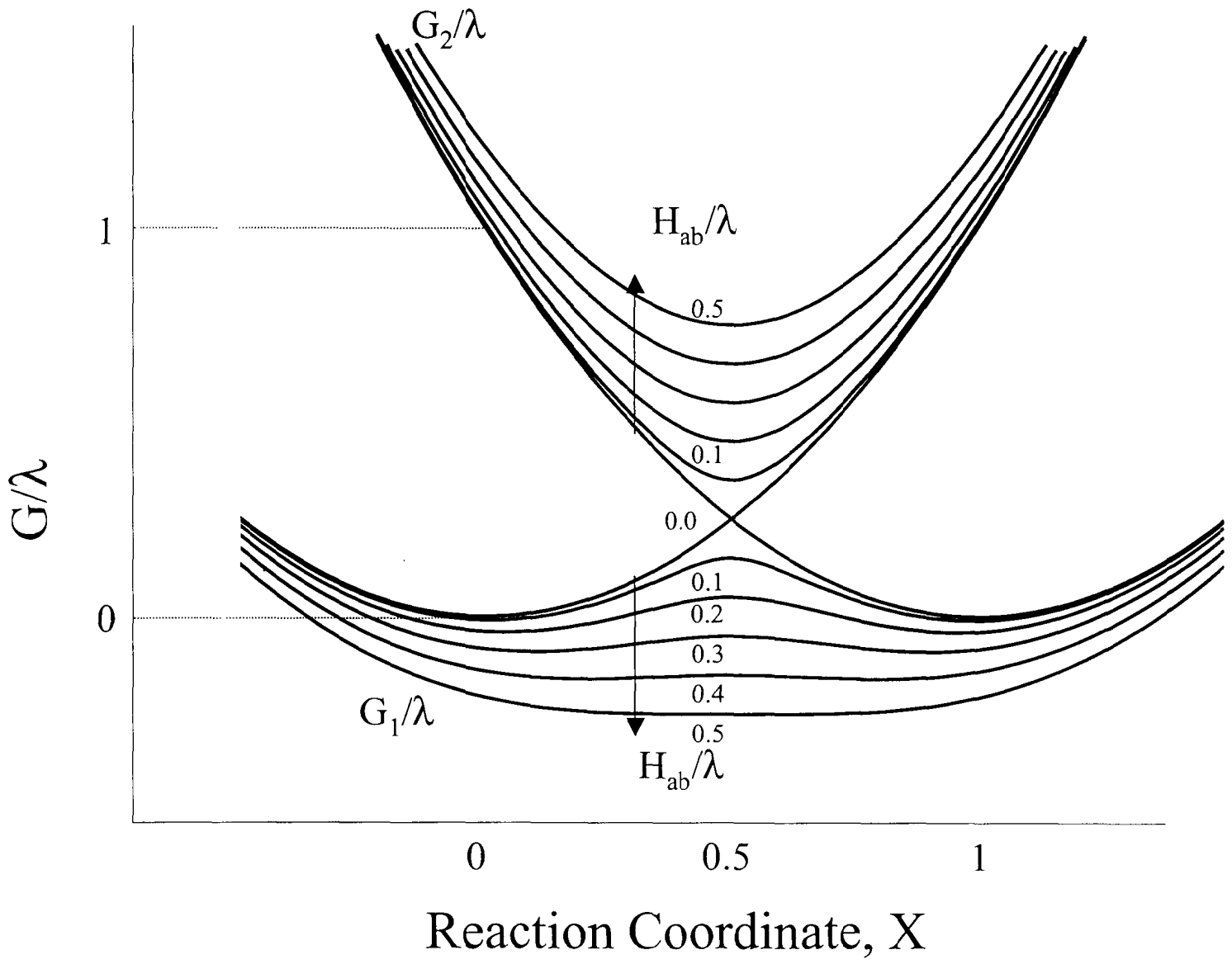
G/λ
1
0
G_2/λ
H_{ab}/λ
0.5
0.1
0.0
0.1
0.2
0.3
0.4
0.5
G_1/λ
H_{ab}/λ
0
0.5
1
Reaction Coordinate, X

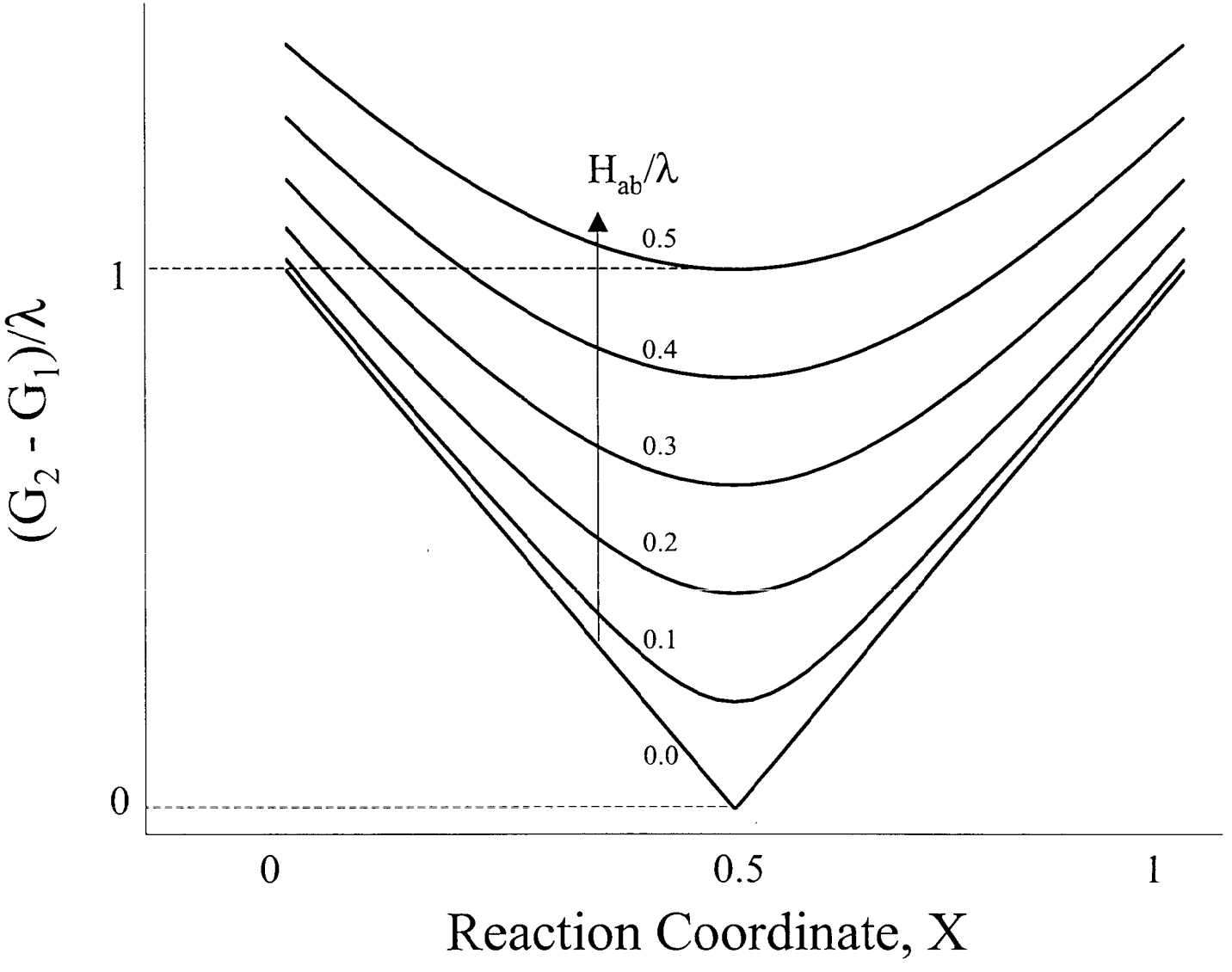
H_{ab}/λ
0.5
0.4
0.3
0.2
0.1
0.0
1
0
$(G_2 - G_1)/\lambda$
0
0.5
1
Reaction Coordinate, X

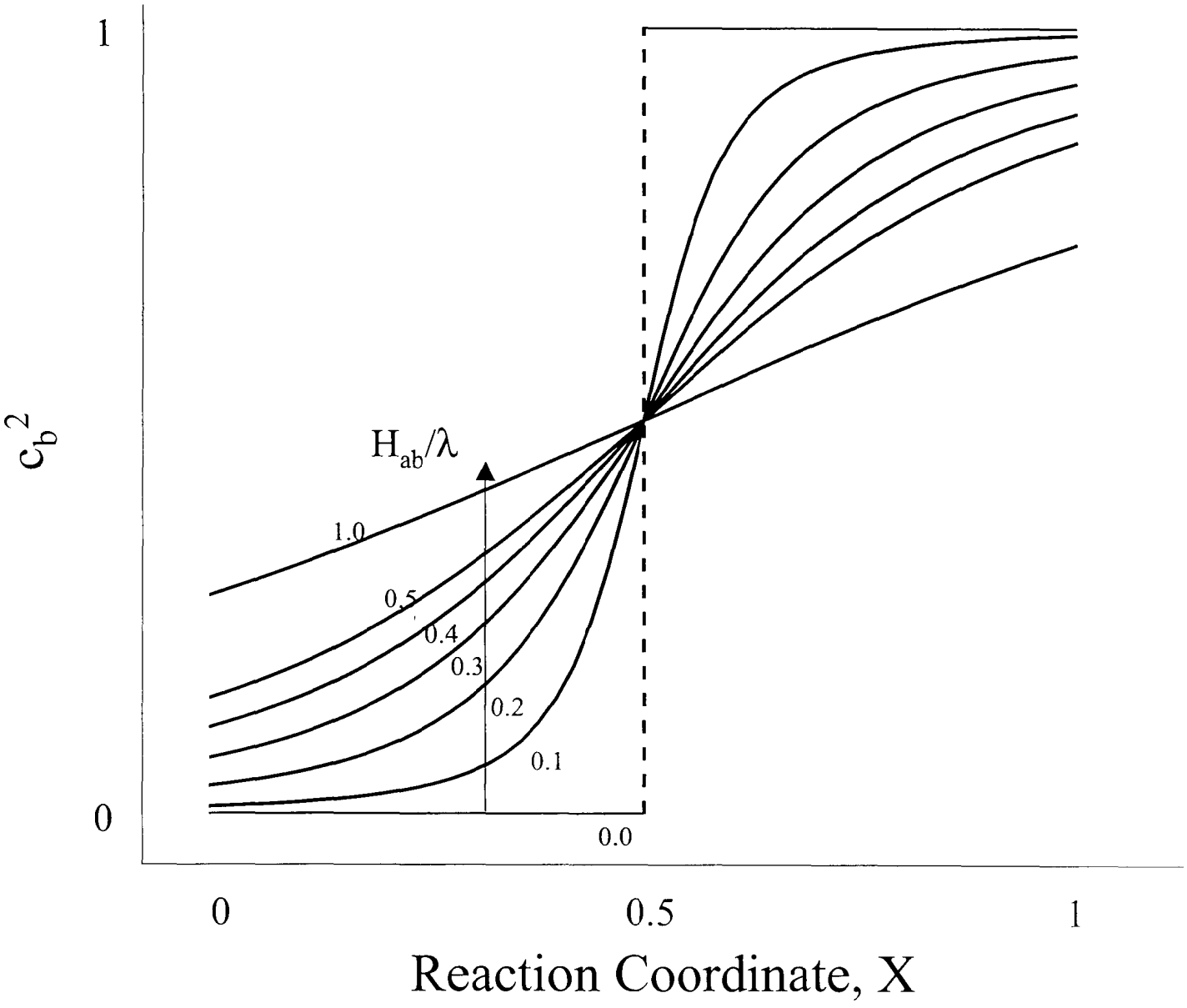
1
0
c_b^2
H_{ab}/λ
1.0
0.5
0.4
0.3
0.2
0.1
0.0
0
0.5
1
Reaction Coordinate, X

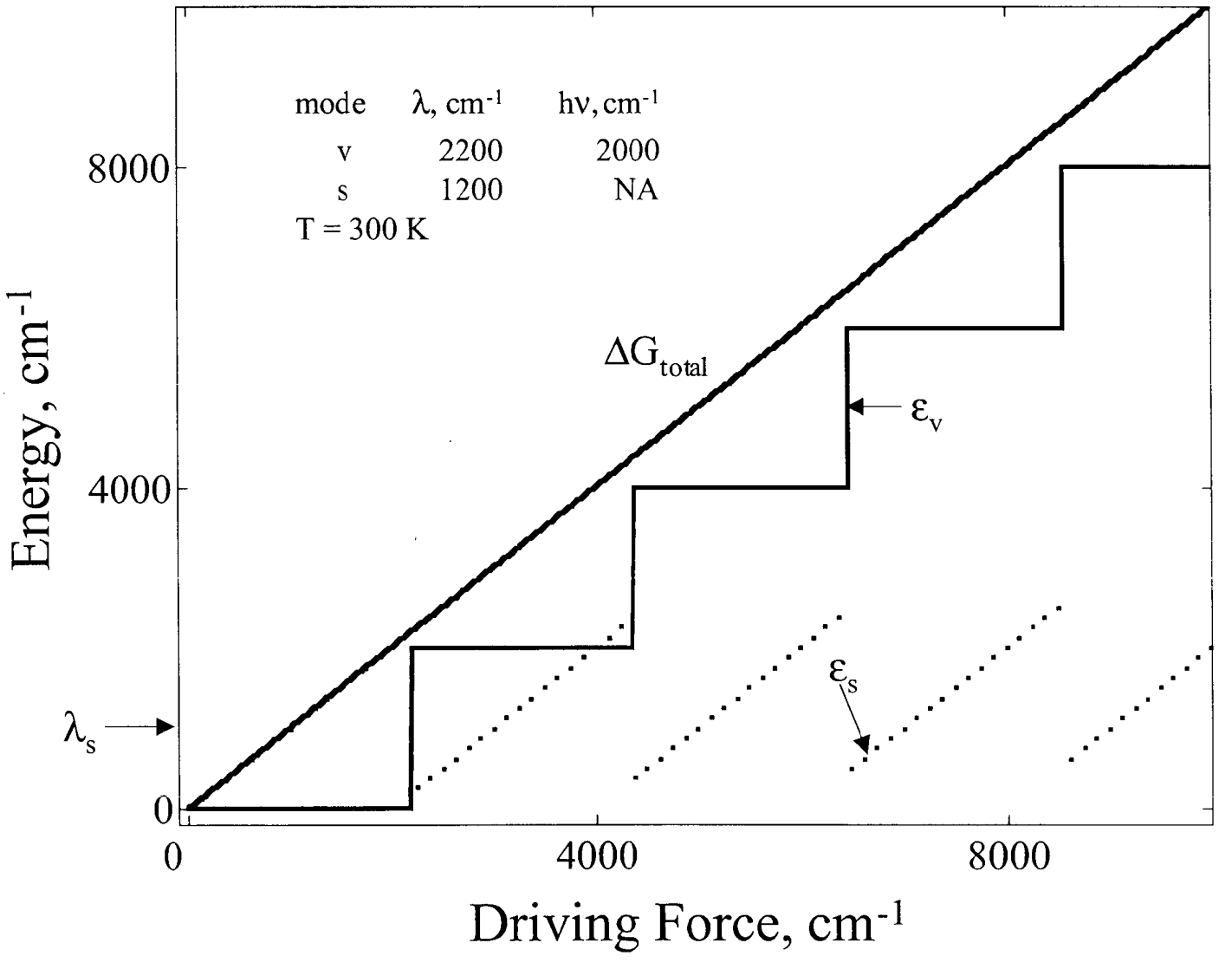
mode λ, cm-1 hν, cm-1
v 2200 2000
s 1200 NA
T = 300 K
8000
4000
0
Energy, cm-1
ΔGtotal
εv
εs
λs
0
4000
8000
Driving Force, cm-1

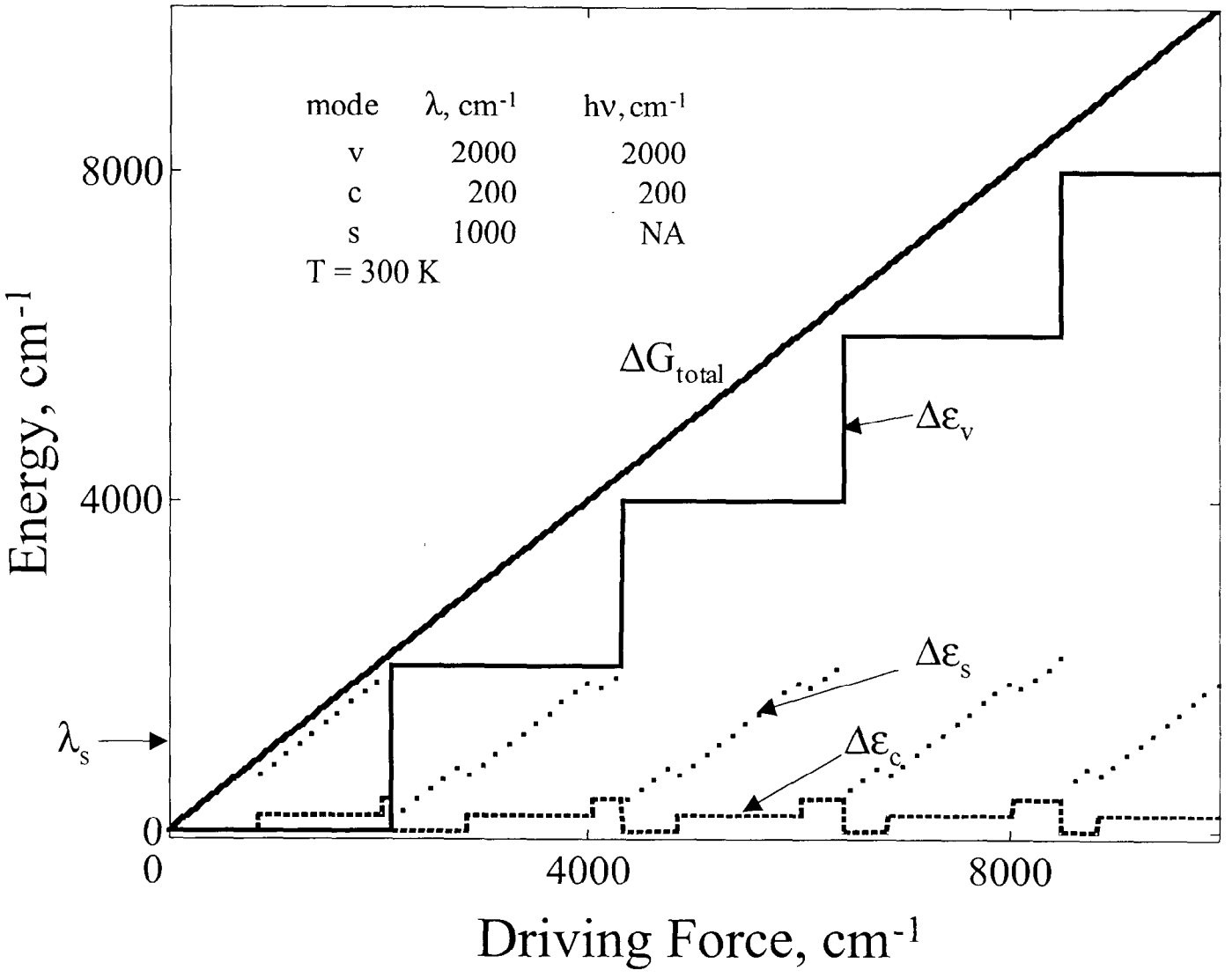
mode λ, cm-1 hν, cm-1
v 2000 2000
c 200 200
s 1000 NA
T = 300 K
ΔG total
Δε v
Δε s
Δε c
λs
8000
4000
0
0
4000
8000
Energy, cm-1
Driving Force, cm-1

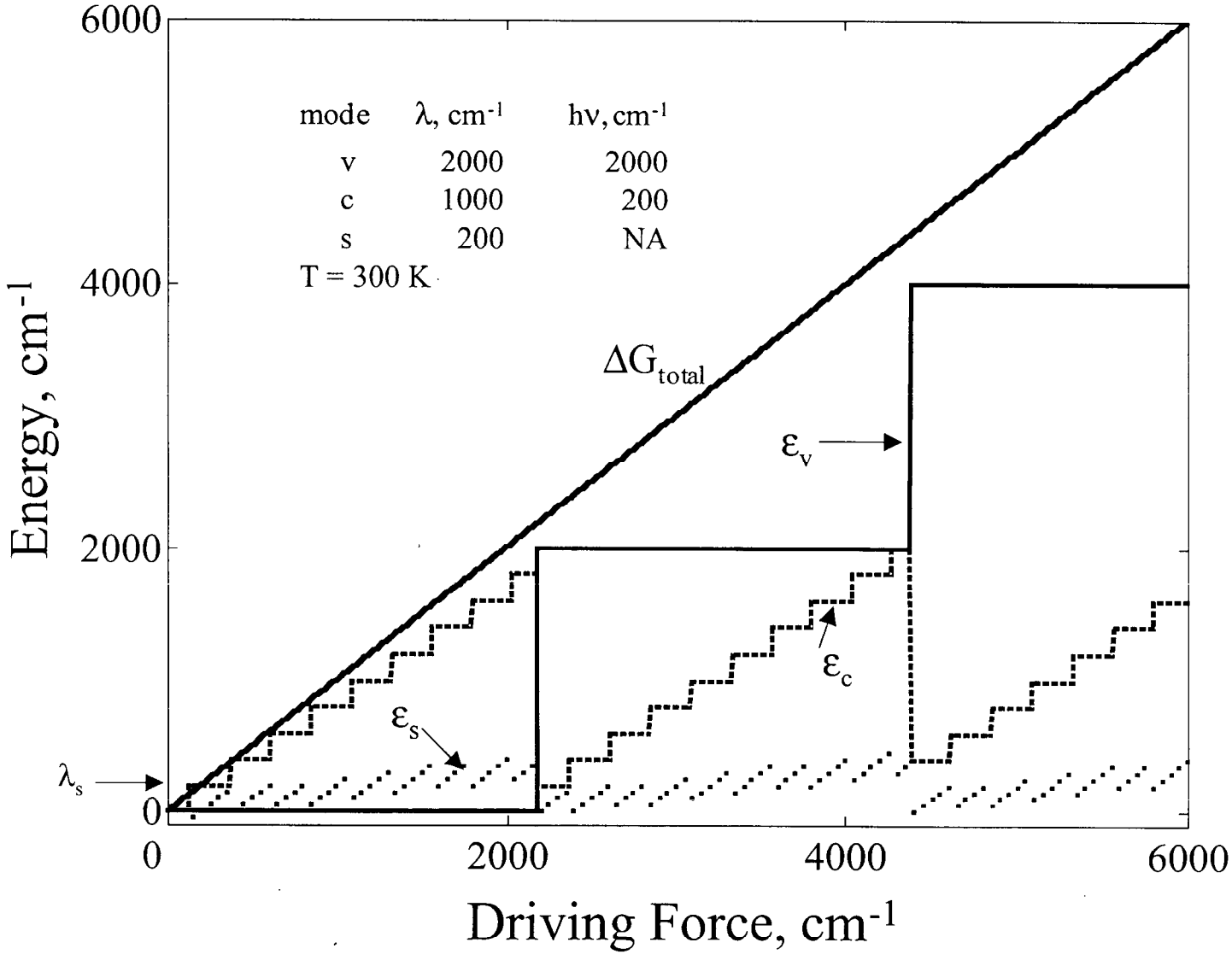
mode λ, cm-1 hν, cm-1
v 2000 2000
c 1000 200
s 200 NA
T = 300 K
ΔGtotal
εv
εc
εs
λs
Energy, cm-1
Driving Force, cm-1
0
2000
4000
6000

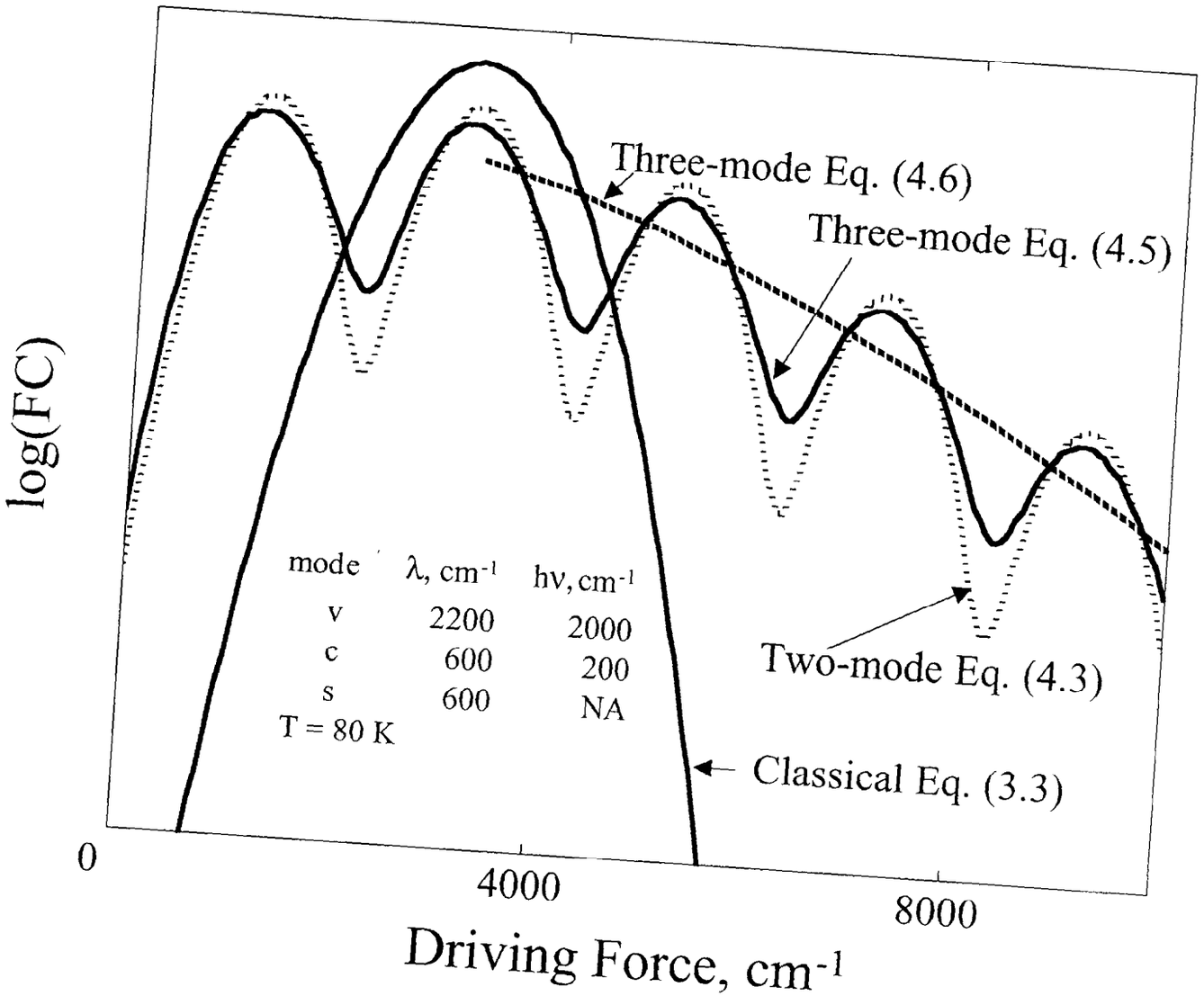
log(FC)
Three-mode Eq. (4.6)
Three-mode Eq. (4.5)
mode λ, cm-1 hν, cm-1
ν 2200 2000
c 600 200
s 600 NA
T = 80 K
Two-mode Eq. (4.3)
Classical Eq. (3.3)
0
4000
8000
Driving Force, cm-1